HDAC inhibitors Tubastatin A and SAHA affect parasite cell division and are potential anti-*Toxoplasma gondii* chemotherapeutics

Carlla Assis Araujo-Silva [a,b], Wanderley De Souza [a,b], Erica S. Martins-Duarte [c,1], Rossiane C. Vommaro [a,b,1,*]

[a] *Laboratório de Ultraestrutura Celular Hertha Meyer - Universidade Federal do Rio de Janeiro - Instituto de Biofísica Carlos Chagas Filho, Av. Carlos Chagas Filho, 373 -Cidade Universitária, Rio de Janeiro - RJ, 21941-170, Brazil*

[b] *Instituto Nacional de Ciência e Tecnologia em Biologia Estrutural e Bioimagens, Universidade Federal do Rio de Janeiro, Brazil*

[c] *Laboratório de Quimioterapia de Protozoários Egler Chiari, Departamento de Parasitologia – ICB – Universidade Federal de Minas Gerais – Avenida Presidente Antônio Carlos, 6.627 –Pampulha - Belo Horizonte, MG, 31270-901, Brazil*

ARTICLE INFO

ABSTRACT

The redirectioning of drugs in the pharmaceutical market is a well-known practice to identify new therapies for parasitic diseases. The histone deacetylase inhibitors Tubastatin A (TST) and Suberoylanilide Hydroxamic Acid (SAHA), firstly developed for cancer treatment, are effective against protozoa parasites. In this work, we aimed to demonstrate the activity of these drugs as potential agents against *Toxoplasma gondii*, the causative agent of toxoplasmosis. TST and SAHA were active against different genotypes of *Toxoplasma gondii*, such as, RH (type I), EGS (I/III) and ME49 (type II) strains. The IC$_{50}$ values for the RH strain were 19 ± 1 nM and 520 ± 386 nM for TST and 41 ± 3 nM and 67 ± 36 nM for SAHA, for 24 and 48 h, respectively. Both compounds were highly selective for *T. gondii* and their anti-proliferative effect was irreversible for 8 days. The calculated selectivity indexes (39 for TST and 30 for SAHA) make them lead compounds for the future development of anti-*Toxoplasma* molecules. Western blotting showed TST led to a significant increase of the nuclear histone H4 and a decrease of H3 acetylation levels. Treatment with 1 μM TST and 0.1 μM SAHA for 48 h decreased the amount of global α-tubulin. Fluorescence and electron microscopy showed that both drugs affected the endodyogeny process impairing the budding of daughter cells. The drugs led to the formation of large, rounded masses of damaged parasites with several centrosomes randomly dispersed and incorrect apicoplast division and positioning. TST-treated parasites showed a rupture of the mitochondrial membrane potential and led to a failure of the IMC assembling of new daughter cells. SAHA and TST possibly inhibit HDAC3 and other cytoplasmic or organelle targeted HDACs involved in the modification of proteins other than histones.

1. Introduction

Toxoplasmosis is a cosmopolitan disease, with high seroprevalence in humans and animals (Dubey et al., 2012). Immunocompromised patients with HIV and pregnant women are among the main risk groups that require more attention, as *Toxoplasma gondii* can traverse the blood-brain and placental barriers. The most severe symptoms include encephalitis and blindness caused by retinochoroiditis; in a foetus, hydrocephalus and mental and motor impairment are significant sequelae (Roberts and McLeod, 1999). The most efficient treatment consists of the concomitant use of pyrimethamine and sulfadiazine, which are active against the tachyzoite stage during the acute phase of the infection, supplemented with leucovorin (folinic acid) to protect against bone marrow suppression (Halonen and Weiss, 2013). Both pyrimethamine and sulfadiazine inhibit folic acid biosynthesis enzymes and can lead to allergy and several adverse effects, making the search for an alternative therapeutic urgent (Montoya and Liesenfeld, 2004).

The redirection of drugs already released on the pharmaceutical market is a well-known practice to identify new therapies for neglected parasitic diseases. Histone deacetylase (HDACs) inhibitors are among

---

* Corresponding author. Laboratório de Ultraestrutura Celular Hertha Meyer - Universidade Federal do Rio de Janeiro - Instituto de Biofísica Carlos Chagas Filho, Av. Carlos Chagas Filho, 373 -Cidade Universitária, Rio de Janeiro - RJ, 21941-170, Brazil.

E-mail addresses: ericamduarte@icb.ufmg.br (E.S. Martins-Duarte), vommaro@biof.ufrj.br (R.C. Vommaro).

[1] Made an equal contribution to the article.

this group of drugs and were first developed for cancer treatment (Gelb et al., 2003; Nwaka and Hudson, 2006), but soon after showed a great variety of effects and perspectives, including anti-protozoan activity (Zuma et al., 2018; Fioravanti et al., 2020). HDACs are responsible for post-translational modifications (PTM) controlling the acetylation status of histones, regulating gene expression and leading to cellular growth arrest (Ruijter et al., 2003). These enzymes also play a major role in the regulation of numerous cytoplasmic protein complexes, including proteins involved in the dynamics of the cytoskeleton (Hubbert et al., 2002; North and Verdin, 2004; Zhang et al., 2009). In terms of structure, function, and localization, HDACs in higher eukaryotes are separated into four classes. Class I (HDAC 1, 2, 3, and 8) has nuclear localization and acts mainly as a transcriptional co-repressor. In Class II (IIa: 4, 5, 7, and 9; IIb: 6 and 10), expression and localization vary according to tissue; this class can be found in the nucleus, cytoplasm, and mitochondria. Class IV has only one member (HDAC 11) and Class III is known as sirtuins (SIRT 1–7) (Suraweera et al., 2018). While classes I, II, and IV contain a zinc-binding site (Ruijter et al., 2003), the sirtuins (class III) require NAD + for their activity (Michan and Sinclair, 2007; Dai and Faller, 2008).

The use of HDAC inhibitors has been shown to be a promising alternative for the treatment of diseases such as malaria (Andrews et al., 2012; Stenzel et al., 2017), trypanosomiasis (Oliveira Santos et al., 2019), schistomiases (Heimburg et al., 2016), and leishmaniasis (Sodji et al., 2014). Previous studies also showed the activity of histone deacetylases inhibitors, such as Apicidin, Valproic acid and Suberoylanilide Hydroxamic Acid (SAHA), against *T. gondii* (Darkin-Rattray et al., 1996; Jones-Brando et al., 2003; Strobl et al., 2007). In *T. gondii*, sequence annotations for five genes of HDAC class I/II [TgHDAC1, TgHDAC2, TgHDAC3, TgHDAC4, and TgHDAC5]) and one gene for a homologue of Sir2 (Saksouk et al., 2005; Vanagas et al., 2012) are found. Previous works showed that TgHDAC3 plays an important role in *T. gondii* cell division (Bougdour et al., 2009), while TgHDAC1 and TgSIR2 play important roles in the process of differentiation of the tachyzoite to bradyzoite stage (Saksouk et al., 2005). In addition, more than 400 acetylation sites have been detected in different *T. gondii* cytoplasmic proteins (Jeffers and Sullivan, 2012), which might be explored to understand their importance to the parasite physiology and to characterize the mode of action of the HDAC inhibitors. SAHA, a selective inhibitor for Class I and II HDAC in mammals, was the first FDA-approved drug for the treatment of cutaneous manifestations such as refractory advanced-stage cutaneous T-cell lymphoma (Grant et al., 2007; Ruefli et al., 2001). Tubastatin A (TST) has been remodeled from Tubacin as an alternative for the treatment of neurodegenerative diseases, as a selective inhibitor of HDAC6 in mammals capable of increasing microtubule stability (Butler et al., 2010).

The present work aims to better explore and compare the effect of these two hydroxamic-acid-derived inhibitors on *Toxoplasma* proliferation and to support these inhibitors of HDAC as lead drugs for the developing of potential treatments for toxoplasmosis.

2. Material and methods

2.1. Host cell and parasites

LLC-MK2 (ATCC©) (epithelial kidney cells from *Macaca mullata*) and Normal Human Neonatal Dermal Fibroblast (NHDF-Neo) (Lonza®) were cultivated as in Martins-Duarte et al. (2008) (Martins-Duarte et al., 2008) RH, RH-RFP (red fluorescence protein), and RH-ACP-YFP (acyl carrier protein-YFP - green apicoplasts); EGS strain (SAG1mCherry/-BAG1sfGFP) and ME49 (GFP), strains of *T. gondii* were cultivated in NHDF fibroblasts and collected after egress.

Compounds: Tubastatin A (TST) (Sigma-Aldrich) and Suberoylanilide Hydroxamic Acid (SAHA) (Sigma-Aldrich) were dissolved in dimethylsulfoxide (DMSO, Merck) in a final concentration of 5 mM. The final concentration of DMSO in the experiments never exceeded

0.1% (v/v).

2.2. Antiproliferative assay

In total, 5×10^5 LLC-MK2 cells were seeded in 24-well plates with coverslips, after 24 h, cells were infected with tachyzoites of RH, EGS or ME49 strains at a ratio of 10:1 parasite/cell for 1 h. Different concentrations of TST and SAHA were added to the infected cells after 6 h. At least 300 cells per coverslip from three independent experiments were scored in a light microscope. The parasite proliferation index was determined as in Martins-Duarte (2006). To calculate IC_{50}, growth curves using the percentage values representing inhibition of parasite growth after treatments relative to the untreated group were analyzed using the non-linear curve, where: $f = min + (max - min)/1 + (x/EC_{50})^{-Hillslope}$ and IC_{50} was the concentration at 50% inhibition of growth. Regression analyses were performed using Sigma Plot 12.0 (Systat Software Inc, Chicago, IL, USA). The activity of TST and SAHA were evaluated against bradyzoites of the EGS strain in 96 h-infected NDHF fibroblasts for 48 h, when the rate of conversion to bradyzoites and spontaneous formation of cysts were higher (Paredes-Santos et al., 2013).

2.3. Cytotoxicity assay in host cells

Cytotoxicity was evaluated by the MTS (3- (4,5-dimethylthiazol-2-yl) -5- (3-carboxymethoxyphenyl) -2- (4-sulfophenyl) -2H-tetrazolium, inner salt) method using LLC-MK2, NDHF fibroblasts, i. p. (intra peritoneal) macrophages, and primary microglial cultures (adapted from Lian et al., 2016) in three independent experiments. In total, 10^4 cells were plated 24 h before the experiment and treated for 48 h. Cytotoxicity was calculated considering the percentage of viable cells. The experimental protocols for animal use were approved by the Institutional Ethics Committee for Animal Use (CEUA/UFRJ: 047/20 and 086/18 for microglia and peritoneal macrophages, respectively).

2.4. Plaque assay

After confluence was reached, NDHF fibroblasts in 25 cm^2 culture flasks were infected with 10^4 parasites and treated with 5 μM TST and 0.2 μM SAHA (IC_{90}) for 5 days. Controls were carried out without any treatment or with medium with 0,1% DMSO. Cells were washed twice with medium and kept for an additional 5 days for recovery. The images were acquired with $16\times$ objective in a Zeiss Zoom v.16 stereo microscope. The area of monolayer disruption was evaluated by the NIH ImageJ software (FIJI). The percentage acquired was considered the control, as 100%. Three independent experiments were performed for each condition.

2.5. Fluorescence assays

Infected cells were fixed for 40 min with 4% formaldehyde in PBS. The samples were permeabilized with 0.5% Triton X-100 (in PBS) for 15 min. Samples were incubated with the following probes: mouse anti-α-tubulin (1:1000; Invitrogen), mouse anti-acetylated α-tubulin (1:1000; Invitrogen), anti-SAG-1 (1:1000; kindly provided by Dr. Dominique Soldati), poly-clonal rabbit anti-Centrin1 (1:1000; Kerafast), polyclonal rabbit anti-acetylated H3 (1:300; Millipore), polyclonal rabbit anti-acetylated H4 (1:500; Abcam), mouse anti-IMC1 (inner membrane complex) Mab45.36 (1:1000; kindly provided by Dr. Ward). Secondary antibodies conjugated with Alexa 488, 546, 568, or 647 (Molecular Probes) at a 1:800 dilution and Hoechst 33,342 at 0.5 μg/mL (Thermo Fisher) were used. For mitochondrial analysis, NDHF fibroblasts infected with RH-ACP-YFP were treated with 1 μM TST or 0.1 μM SAHA for 24 h. The cells were incubated with 50 nM MitoTracker™ Red CMXRos (Invitrogen™) for 45 min. Samples were imaged with an LSM 710

Table 1
Selective Indexes for different cell types after treatment with TST and SAHA for 48h.

Compounds	*T. gondii* EGS	*T. gondii* RH	Cell Types								
			LLCMK2		Macrophages		NDHF		Primary microglial		
	IC_{50} [μM]	IC_{50} [μM]	aCC50 [μM]	[b]SI^c	[a]CC_{50} [μM]	SI^c	[a]CC_{50} [μM]	SI^c	[a]CC_{50} [μM]	SI^c
TST	0.29	0.52	>20	>38	13.50	26	>20	>39 [d]>69	>20	>39
SAHA	0.04	0.07	5.94	89	4.61	68	>20	>30 [d]>500	>20	>30

[a] CC_{50}: Concentration necessary to kill 50% of the cells.
[b] SI: Selective index = CC_{50}/IC_{50}.
[c] Calculated with IC_{50} of the RH strain.
[d] Calculated with IC_{50} of the EGS strain (atypical).

module and SR-SIM (Super-Resolution Structured Illumination Microscopy) using the Zeiss Elyra PS.1 and by Axiobserver Zeiss microscope. The images were processed using ZEN Black (Zeiss, Germany). All the fluorescence assays were carried out in two independent experiments. Quantification of parasite masses was performed with tachyzoites of RH strain after treatment with 1 μM TST and 0.1 μM SAHA for 24 h and labeled with anti-SAG-1. The results are the average of three independent experiments; statistical analysis was performed with One-Way ANOVA, Sidak's multiple comparisons test, $P < 0.05$.

2.6. Western blotting

Infected NDHF fibroblasts were treated with SAHA and TST for 48 h, then scraped and lysed through passages in a 30G needle syringe, lysed cells were centrifuged at 2000 rcf for 10 min and resuspended in PBS and passed through an 8-μM filter to purify the tachyzoites. In total, 10^6 parasites in a 10-μL lysis buffer containing a 0.1% protease inhibitor cocktail (Sigma) were cryolysed. Membranes were incubated with anti-α-tubulin (1:1000), anti-acetylated α-tubulin (1:2000), anti-Histone H3 (1:1000, CellSignaling), anti-acetylated Histone H3 (Lys 9/14) (1:1000, Santa Cruz), anti-Histone H4 (1:3000, CellSignaling) or anti-acetylated Histone H4 (Lys 16) (1:1000, Sigma) for 1 h depending of the assay. GAPDH was used as the loading control (1:2500, Abcam). Membranes were incubated with peroxidase-conjugated anti-mouse or anti-rabbit IgG (Promega) 1:4000 in TBS-T. Membranes were then exposed to an enhanced chemiluminescence (ECL) reagent (Promega) and visualized using the ImageQuant LAS 500 (GE Healthcare Life). Quantification of band intensities from three independent experiments was performed with the NIH ImageJ software. The normalization of the amount of protein was performed using the loading control in all quantitative analyzes. The ratio of rTubac/rTub, rH3ac/rH3 and rH4ac/rH4 for each treatment was also carried out.
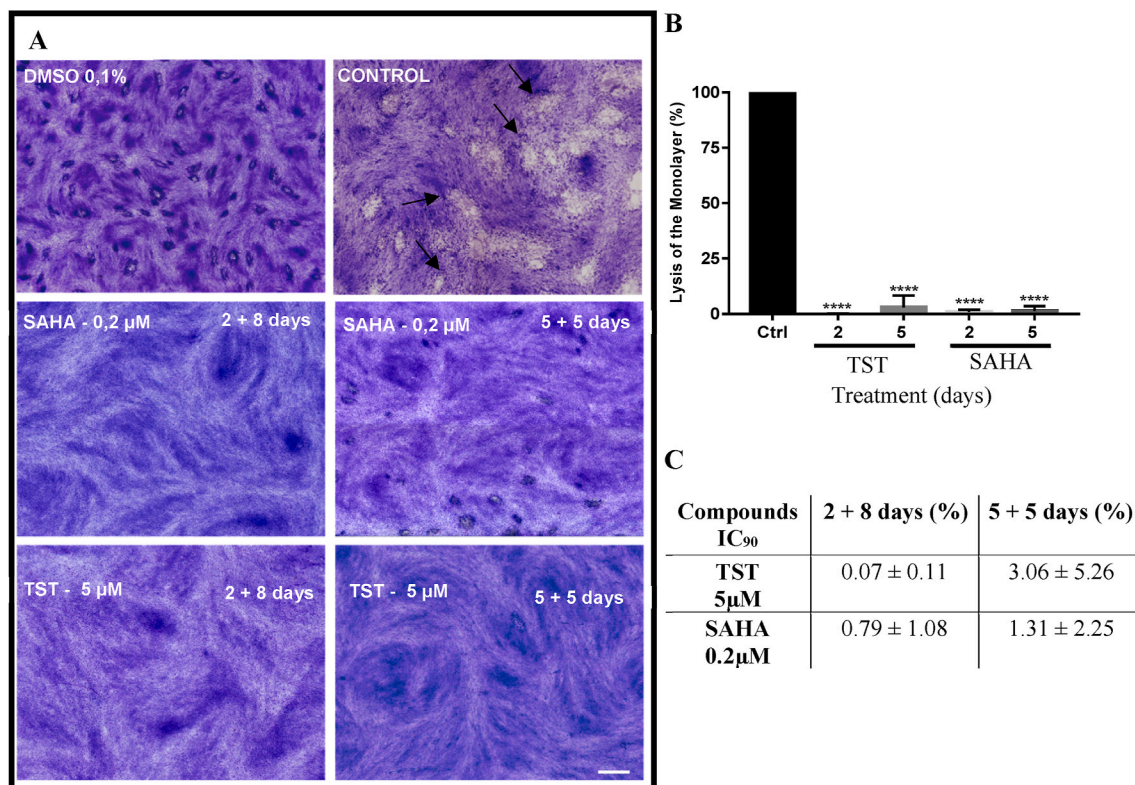

Fig. 1. Plaque Assays after TST and SAHA treatment. A NDHF fibroblasts monolayers were infected with 10^4 tachyzoites. Treatment was performed with 5 μM TST or 0.2 μM SAHA for 2 or 5 days. At the end of treatment, cells were incubated with fresh medium for 8 days (2 days + 8 days) or 5 days (5 days + 5 days). B and C show the percentage of lysis of the monolayers. 1 mm scale bar. Statistical analysis was performed with One-Way ANOVA, Bonferroni's multiple comparison test, **** <0.0001, $P < 0.0001$, n3.
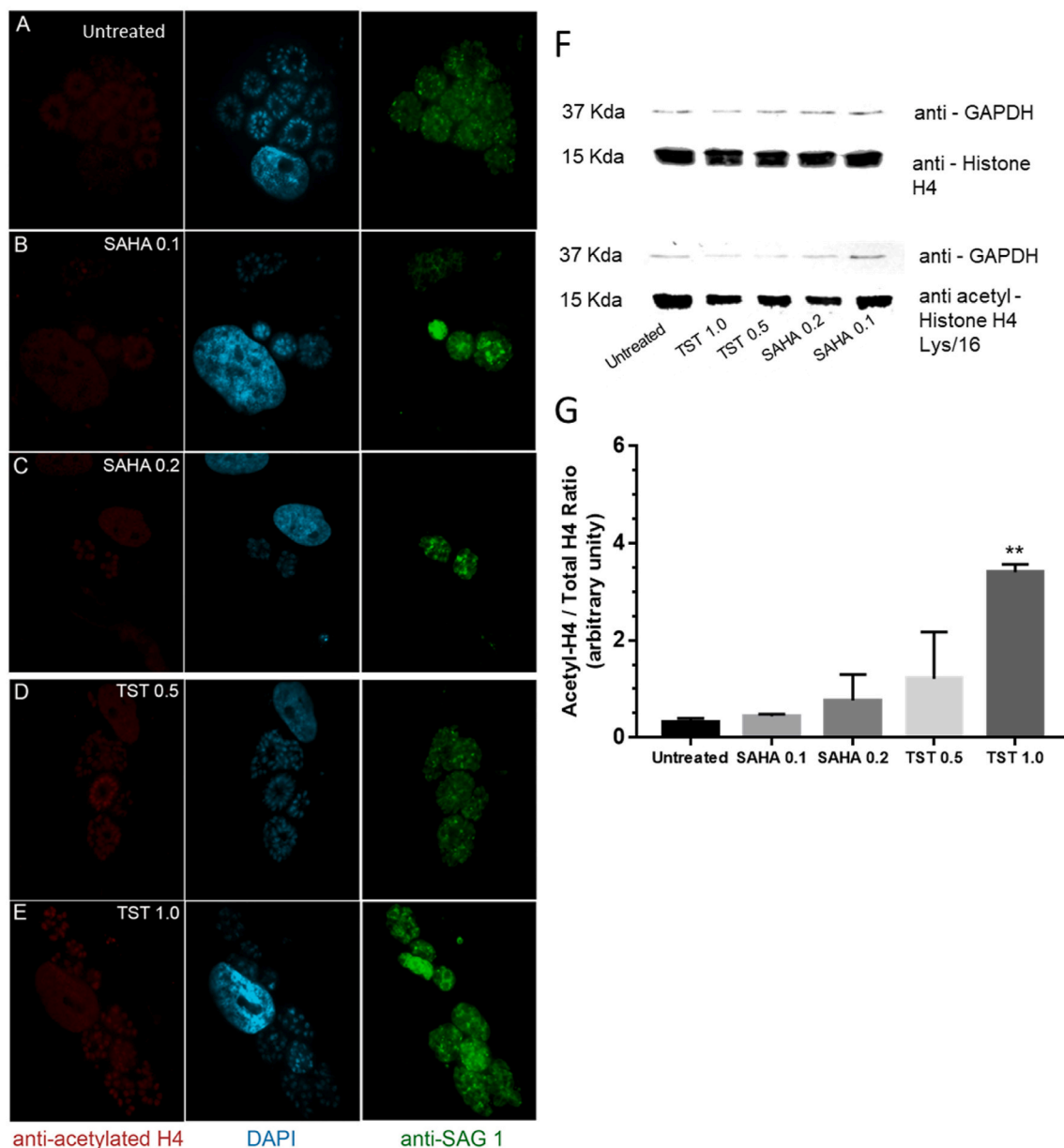
Compounds IC_{90}	2 + 8 days (%)	5 + 5 days (%)
TST 5μM	0.07 ± 0.11	3.06 ± 5.26
SAHA 0.2μM	0.79 ± 1.08	1.31 ± 2.25

Fig. 2. Effect of TST and SAHA in the acetylation levels of histone H4 in *T. gondii* after 48 h of treatment. A-E Immunofluorescence analysis of the acetylated H4 labeling of tachyzoites treated with SAHA and TST. Tachyzoites were labeled with anti-acetylated H4 (red), anti-SAG-1 (green), and DAPI (blue). F Western blot labeled with anti-H4 and anti-acetylated-H4/Lys16. G The relativization of rH4ac/rH4. Statistical analysis was performed using one-way ANOVA and Dunnett's multiple comparisons test. F ** 0.0048, $P < 0.05$. (For interpretation of the references to colour in this figure legend, the reader is referred to the Web version of this article.)

2.7. Effect of SAHA and TST on the T. gondii ultrastructure

LLC-MK$_2$ or NDHF fibroblasts were infected with tachyzoites at a ratio of 10:1 parasite/cell. After 6 h of interaction, the compounds were added at concentrations 5-fold higher than the 24 h-IC$_{50}$ values. Cells were fixed with 2.5% glutaraldehyde and carried out as in Martins-Duarte et al. (2008). Ultrathin sections from three independent experiments were stained with uranyl acetate and lead citrate and observed in a Jeol 1200 EX (Jeol LTD, Tokyo, Japan).

2.8. Statistical analysis

Statistical analysis of the data was performed using GraphPad Prism software. Results with $P < 0.05$ were considered statistically significant.

3. Results

3.1. Antiproliferative effect of TST and SAHA against different strains of T. gondii

The effects of TST and SAHA against tachyzoites of the RH strain (type I) were analyzed for 24 and 48 h of treatment. Both compounds showed high efficacy (Table 1 and Supplementary data 1) and inhibited *T. gondii* proliferation with concentrations at the nanomolar range. IC$_{50}$ calculations showed values of 19 ± 1 nM and 520 ± 386 nM for TST and 41 ± 3 nM and 67 ± 36 nM for SAHA after 24 h and 48 h, respectively. Treatment of infected cultures with TST, for 48 h, presented a value of IC$_{50}$ significantly higher than for 24 h. Both drugs also showed activity against the Brazilian atypical strain EGS. IC$_{50}$ calculations showed values of 290 ± 66 nM for TST and 44 ± 11 nM for SAHA after 48 h,
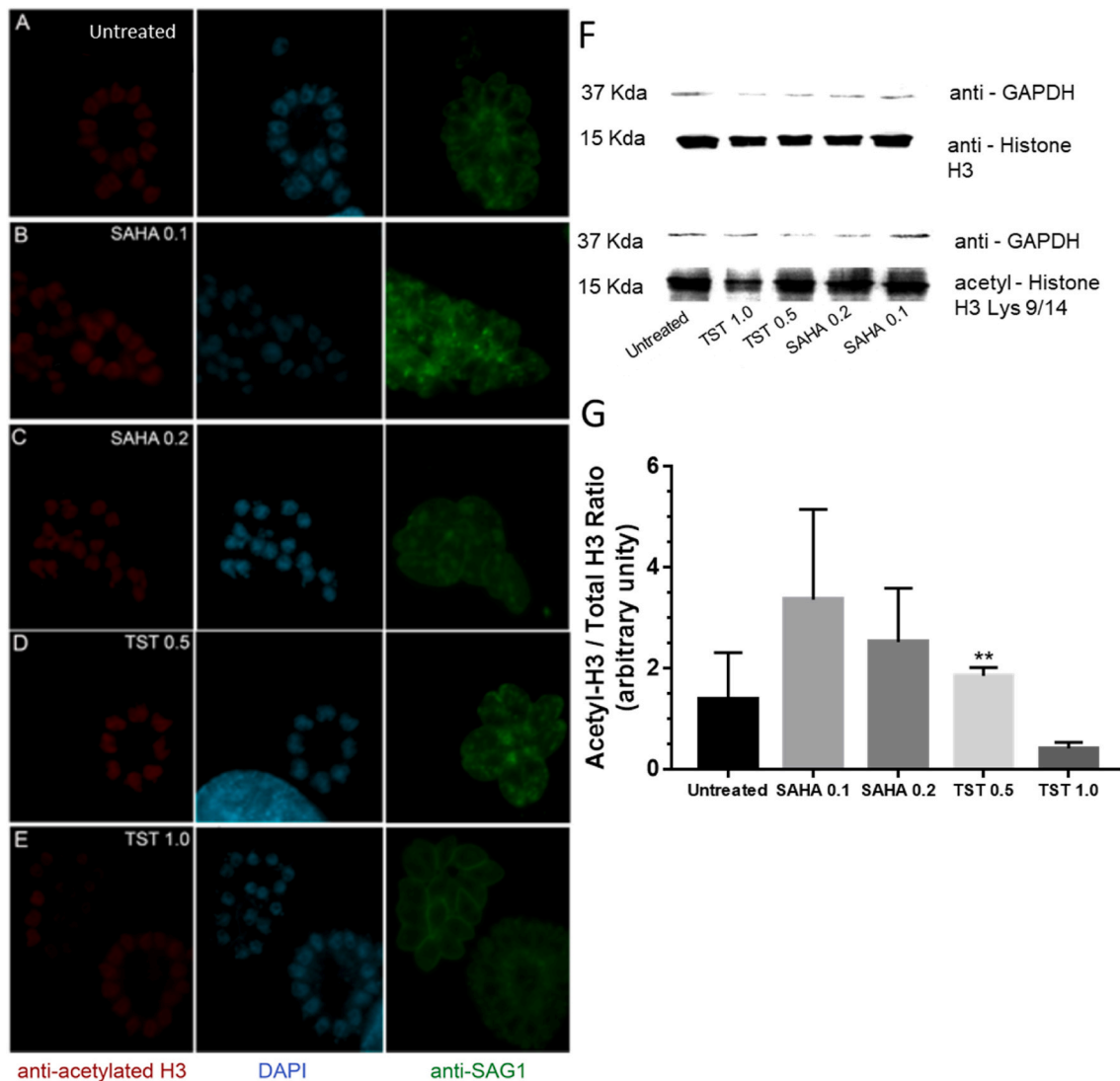
Fig. 3. Effect of TST and SAHA in the acetylation levels of histone H3 in *T. gondii* after 48 h of treatment. A-E Immunofluorescence analysis of the acetylated H3 labeling of tachyzoites treated with SAHA and TST. Tachyzoites were labeled with anti-acetylated H3 (red), anti-SAG-1 (green), and DAPI (blue). F Western blot labeled with anti-H3 and anti-acetylated-H3/Lys 9/14. G The relativization of rH3ac/rH3. Statistical analysis was performed using one-way ANOVA and Dunnett's multiple comparisons test. F** 0.0048, $P < 0.05$. (For interpretation of the references to colour in this figure legend, the reader is referred to the Web version of this article.)

respectively (Table 1 and Supplementary data 1).

TST and SAHA also showed activity against the bradyzoite form of the EGS strain after 48 h of treatment; 1 and 5 μM TST and 0.1 μM SAHA inhibited significantly the proliferation or viability of bradyzoites. Treatment with 0.2 μM SAHA maintained the same amount of bradyzoites in the culture as in the control (Supplementary data 2).

In order to confirm the selective effect of compounds, a cytotoxicity assay was performed against LLC-MK2, NDHF fibroblasts, i. p. macrophages, and primary microglial cultures for 48 h (Table 1). TST and SAHA were tested in the following concentrations: 0.1, 1.0, 5.0, 10.0 and 20.0 μM. Both compounds showed a selective effect in inhibiting *T. gondii* proliferation compared to different host cells, as effective concentrations for parasites did not affect host cells. Higher selective indexes were obtained for NDHF fibroblasts, a mixed culture of mouse astrocytes/microglia, and LLC-MK$_2$ in comparison to mouse peritoneal macrophages, which showed less tolerability with CC$_{50}$ of SI of 13 μM and 26, respectively, for TST and 4.6 μM and 69, respectively for SAHA. Cytotoxicity analysis in NDHF fibroblasts after treatment for 120 h with higher concentrations (20–80 μM) of SAHA and TST showed CC$_{50}$ of 6.5 μM and 29.9 μM, respectively (Supplementary data 3).

To verify whether TST and SAHA effects were reversible for parasite viability, plaque assays were carried out. NDHF fibroblasts infected with 10^4 tachyzoites were treated with 5 μM TST and 0.2 μM SAHA for 2 or 5 days. At the end of treatment (Fig. 1), cells were washed and incubated with medium without drugs for 8 days (2 days + 8 days) or 5 days (5 days + 5 days). Both compounds significantly prevented parasite proliferation and protected the integrity of the monolayer, even when the drugs were removed (Fig. 1A). Quantification of the plaque assay showed that lysed areas in treated monolayers represented just 3% of the lysed total area found for untreated infected monolayers (Fig. 1B and C). Pre-treatment of the NDHF fibroblasts for 2 or 5 days with both drugs did not prevent the parasite entry or proliferation (Data not shown).

3.2. Effect of SAHA and TST on T. gondii H3 and H4 histone acetylation

Considering that SAHA, a non-specific inhibitor of HDCA and TST, a high selective inhibitor for mammal HDAC6, we first evaluated how different effective concentrations of both compounds affected histone H4 and H3 acetylation levels in *T. gondii* nucleus, after 48 h treatment. Analysis of the densitometry of the Western blot showed that 0,2 μM
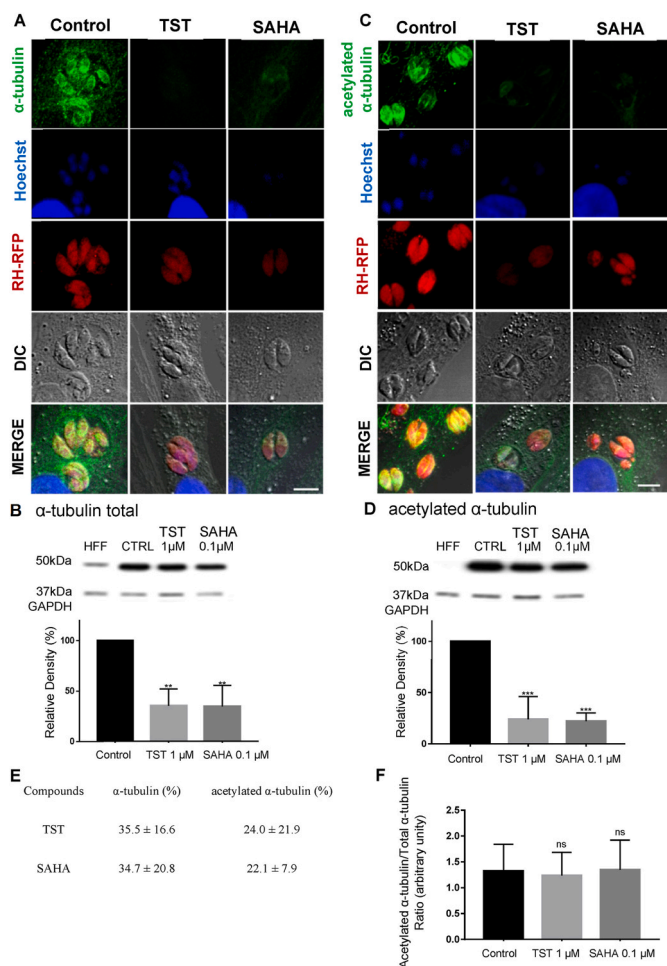
Fig. 4. Effect of TST and SAHA on parasite microtubules. A-B Immunofluorescence and Western blotting labeled with α-tubulin. C-D labeled with α-acetylated tubulin after TST 1 μM and SAHA 0.1 μM treatment. Immunofluorescence assays were performed using RH-RFP (red fluorescence protein) tachyzoites, after 24 h treatment. 5 μm scale bar. Western blots were performed after 48 h treatment. E Quantification of α-tubulin and acetylated α-tubulin in percentage. Statistical analyses were performed using One-Way ANOVA, Bonferroni multiple comparison test, B **0.0043, $P < 0.05$; D ***0.0009, $P < 0.05$, n3. F Ratio of acetylated/total tubulin. Three independent experiments were performed in triplicate. Statistical analysis was performed using One-Way ANOVA, Bonferroni multiple comparison test, B **0.0043, $P < 0.05$; D ***0.0009, $P < 0.05$. NS- not significant. (For interpretation of the references to colour in this figure legend, the reader is referred to the Web version of this article.)

SAHA caused modest increase in the acetylation levels of both H4 (lys16) and H3 (Lys 9/14). On the other hand, 1 μM TST led to a significant increase in acetylation levels in H4 (lys16), but to a decrease below the levels of the untreated cells for H3 (Lys 9/14) (Figs. 2G and 3G). The same acetylation pattern could be observed in the fluorescence images, where 1 μM TST decreased the intensity labeling of acetylated H3 (Fig. 3E). Western blot results were obtained as the ratio of each protein - H4ac/H4 or H3ac/H3 (Figs. 2 and 3).

3.3. Effect of SAHA and TST on parasite tubulin

TST is a selective HDAC6 inhibitor involved in the acetylation state of microtubules in mammalian cells and SAHA is an HDAC inhibitor, which also interferes with the levels of tubulin acetylation. Thus, we analyzed the effects of TST and SAHA on the acetylation levels of the *T. gondii* tachyzoite microtubules (Fig. 4). For that, NDHF fibroblasts
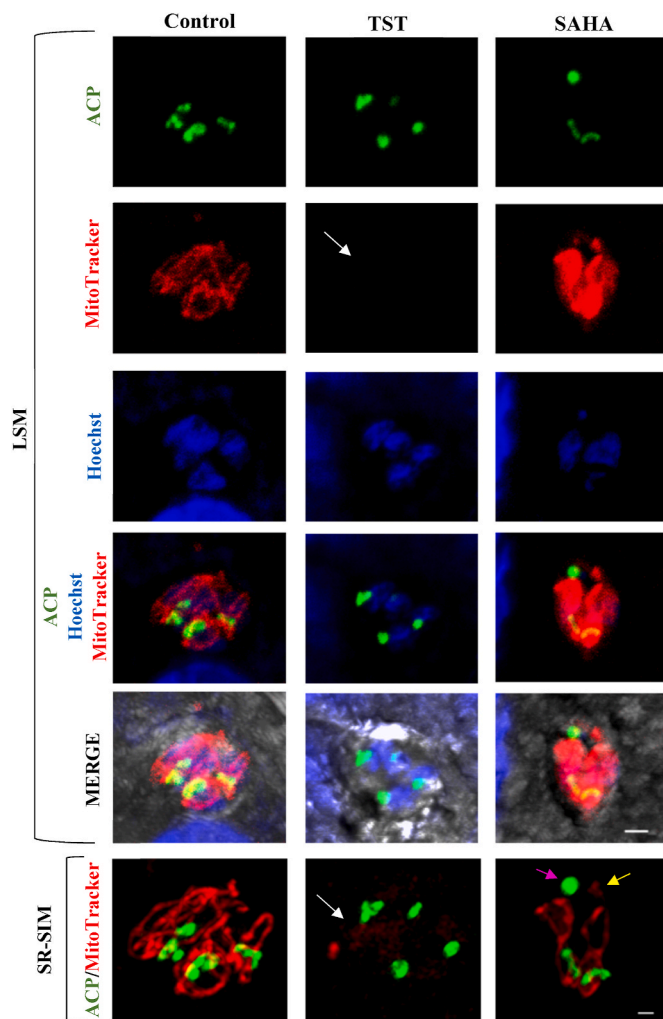

Fig. 5. Effect of TST and SAHA on parasite mitochondrial membrane potential and mitochondrial partitioning. RH-ACP-YFP tachyzoites-infected NDHF fibroblasts treated with 1 μM TST or 0.1 μM SAHA for 24 h were incubated with the mitotracker fluorescent probe. Reduction in mitochondrial membrane potential can be seen (white arrow) after TST treatment; and mitochondrial fragmentation (yellow arrow) and ball-shaped apicoplast formation (purple arrow) after SAHA treatment. LSM, 2 μm scale bar; SR-SIM, 1 μm scale bar. (For interpretation of the references to colour in this figure legend, the reader is referred to the Web version of this article.)

infected with RH-RFP were incubated with 1 μM TST and 0.1 μM SAHA for 24 h. After treatment, the cells were labeled with anti-α-tubulin or anti-acetylated α-tubulin and analyzed by fluorescence microscopy (Fig. 4A and C). The images showed a decrease in the staining intensity of tubulin and acetylated tubulin (Fig. 4A and C). Western blotting analysis of parasites treated with 1 μM TST and 0.1 μM SAHA for 48 h showed a similar effect (Fig. 4B and D). There was no change in tubulin acetylation levels when the ratio - rTubac/rTub - was performed for both compounds (Fig. 4F). There was significant decrease in the global α-tubulin after both treatments (Figure B–D).

3.4. Effects of TST and SAHA on parasite mitochondria

NDHF fibroblasts infected with RH-ACP-YFP tachyzoites was treated with 1 μM TST and 0.1 μM SAHA for 24 h and incubated with 50 nM Mitotracker. In control cells, mitochondria appeared in one of their typical "loop" stages and associated with the apicoplast (Fig. 5 SR-SIM control). After TST treatment, a reduction of the labeling intensity of mitochondria could be observed (Fig. 5). The mitochondrion structure
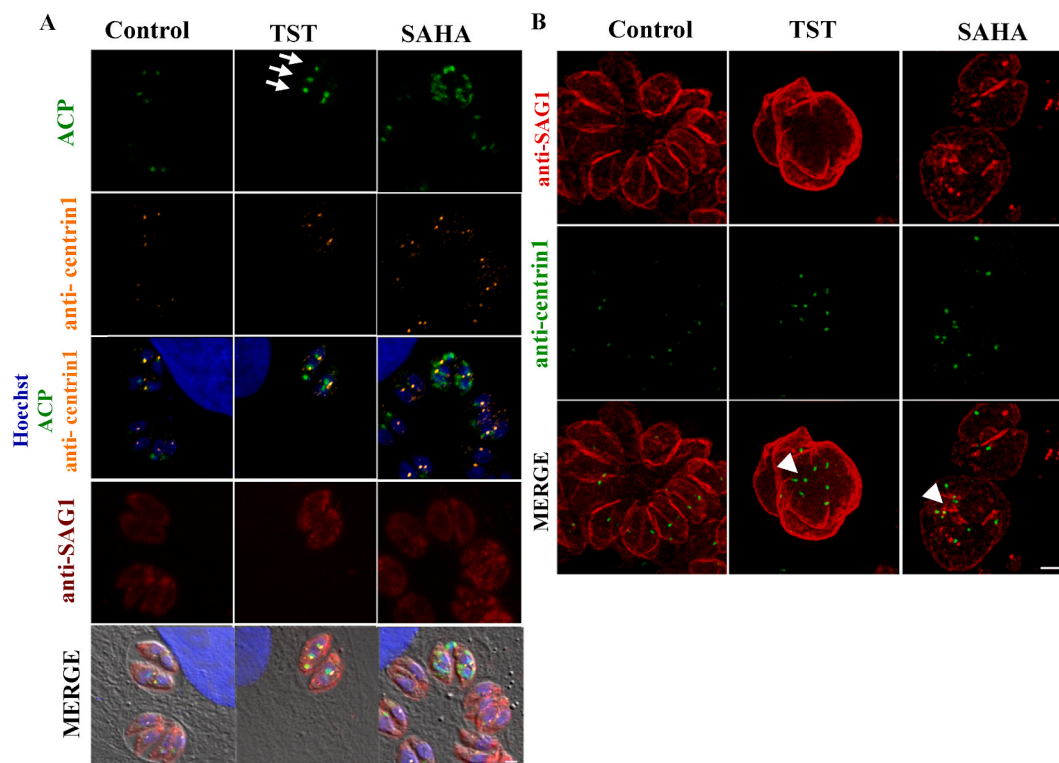
Fig. 6. Effect of TST and SAHA on parasite apicoplast by Immunofluorescence. Effect of SAHA and TST. RH-ACP-YFP tachyzoites were treated with TST (1 μM) or SAHA (0.1 μM) for 24 h were labeled with anti-SAG1 and anti-Centrin1. Control parasites presented normal morphology and only one centrosome and apicoplast. Treatment with TST and SAHA affected apicoplast partition and led to organelle fragmentation (white arrows). 2 μm scale bar. B 3D SR-SIM projection of NDHF fibroblasts infected with the RH strain. Treatment with both compounds led to the interruption of daughter cells' budding process. Several centrosomes randomly dispersed in the round masses of damaged parasites are clearly seen (arrowheads). 2 μm scale bar.

was also affected, as it did not present the tubular and branched shape. Treatment with SAHA seemed to lead to mitochondrion fragmentation (Fig. 5). Altogether, these data may indicate a rupture of the membrane potential.

3.5. Effects of SAHA and TST on cell division and apicoplast

As the treatment affected the amount of parasite tubulin, we verified whether the compounds affected parasite replication. For that, infected NDHF fibroblasts were labeled with anti-SAG-1 (for parasite pellicle) and anti-centrin1 (for centrosome). While untreated parasites showed normal morphology and contained only one centrosome per parasite (Fig. 6A), treatment with 1 μM TST for 24 h (Fig. 6B) induced the formation of a rounded mass of parasites showing disruption of the daughter cell budding process (Fig. 6B TST) and the presence of several centrosomes (Fig. 6B TST). After treatment with 0.1 μM SAHA, the effect on parasites was even more drastic, as seen by the presence of masses of damaged parasites showing several centrosomes and mislocalization of this structure at the periphery of the mass of parasites (Fig. 6B SAHA).

Considering that treatment with SAHA altered apicoplast acetylation, and keeping in mind the role that centrosomes play in the correct apicoplast partitioning in daughter cells during *T. gondii* endodyogeny (Striepen et al., 2000), we evaluated the effects of the treatment in this organelle. Cells infected with ACP-YFP tachyzoites were labeled with anti-SAG1 and anti-centrin1 in fluorescence. Untreated parasites showed normal morphology and contained just one apicoplast (Fig. 6A). However, tachyzoites treated with 0.1 μM SAHA showed apicoplast fragmentation (Figs. 6A and 5). Analysis with SR-SIM confirmed that apicoplast division was affected by SAHA (Fig. 5).

Alteration at the apicoplast partition was seen in parasites treated with TST (Fig. 6A). The disruption of the budding process of daughter cells and the consequential formation of a rounded mass of parasites

were also seen with anti-IMC1 labeling after TST treatment (Fig. 7 LSM and SR-SIM). The IMC (inner membrane complex) appeared only partially assembled in circumscribing each new damaged daughter cell and the plasma membrane appeared to not be associated with IMC in several parasitophorous vacuoles, possibly impairing the individualization of the new parasites. Treatment with SAHA induced the formation of masses of parasites, although the assembling of IMC was not complete (Fig. 8). The quantification of parasitophorous vacuoles containing masses of parasites from fluorescence assays of Figs. 6 and 7 can be seen in the Supplementary data 5. The effects of 1 μM TST and 0.1 μM SAHA treatments for 24 h was also evaluated against tachyzoites of the ME49 strain (type II). Both treatments were able to inhibit tachyzoite proliferation significantly and led to the formation of masses of damaged parasites or anomalies in the endodyogeny process (Supplementary data 4 A and 4 B).

To determine the action of the compounds on the parasite ultrastructure, infected NDHF fibroblasts treated with 0.2 μM SAHA and 3 μM TST were analyzed by TEM for 12, 24, and 48 h. While untreated parasites formed a rosette with typical morphology and ultrastructure (Fig. 8A, D, and 8G), treatment with both compounds led to abnormalities in the endodyogeny process, with the appearance of large parasites (Fig. 8B, E, and 8I). TST treatment led to mitochondrion with disrupted crista (Fig. 8B and H). After SAHA treatment, tachyzoites showed apicoplasts with an unusual morphology and apparent fragmentation (Fig. 8C) and the appearance of myelin-like figures (Fig. 8F).

4. Discussion

Herein, we show that compounds of the hydroxamic acid family, such as SAHA, an inhibitor for classes I and II HDACs in mammals, and TST, selective for HDAC6 (Ruefli et al., 2001) in mammals, are active against tachyzoites of different genotypes of *Toxoplasma gondii*, such as,
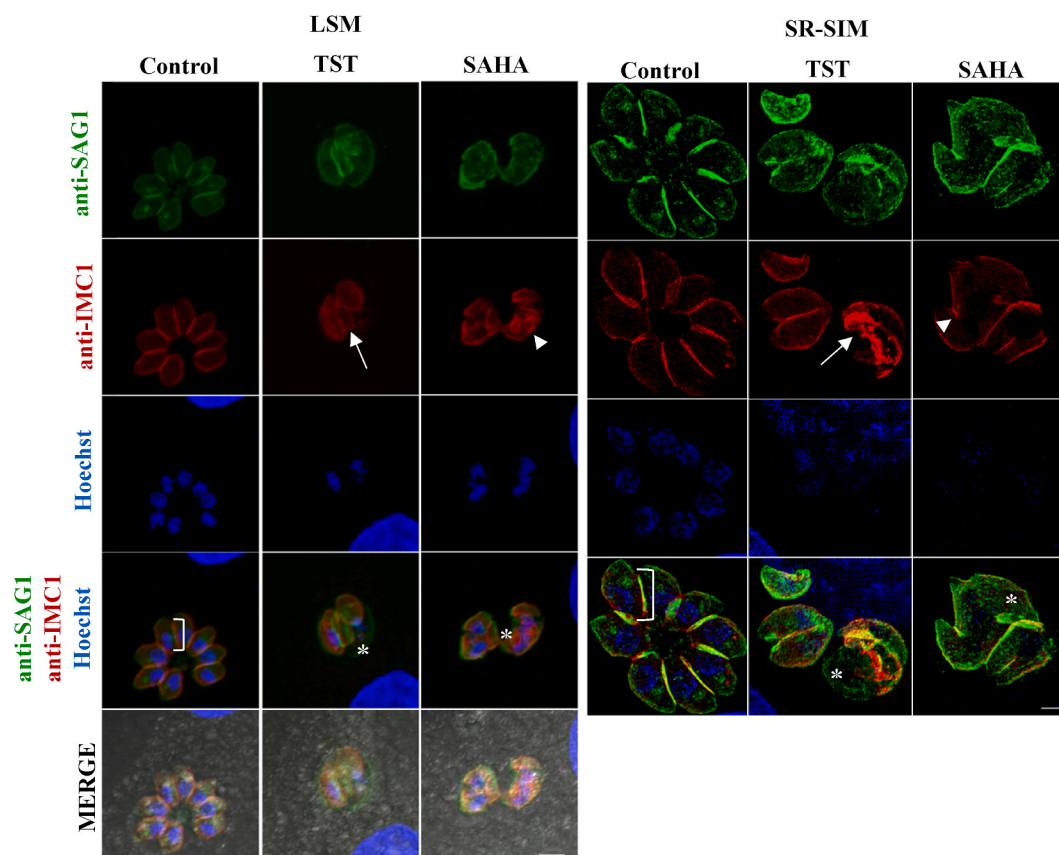
Fig. 7. Effect of TST and SAHA on parasite inner membrane complex. Immunofluorescence analysis showing NDHF fibroblasts infected with RH strain treated with 1 μM TST or 0.1 μM SAHA for 24 h. Treated cells were labeled with anti-IMC1. Control tachyzoites formed characteristic rosettes with completely assembled IMC (bracket), whereas the IMC in TST treated parasites was drastically disorganized (white arrow). SAHA treatment revealed incomplete IMC assembly (arrowhead) and both compounds led to the formation of a mass of damaged parasites (asterisk). 2 μm scale bar.

RH (type I), EGS (atypical) and ME49 (typeII) strains. In agreement with the previous study of Strobl and colleagues [83 nM] (Strobl et al., 2007), SAHA exhibited IC$_{50}$ against *T. gondii* at nanomolar range. SAHA showed activity at a nanomolar range also against other parasites, as *Plasmodium falciparum, P. knowlesi, Trypanosoma brucei* (Chua et al., 2017; Engel et al., 2015). Data on the activity of TST are reported for the first time in this study. Similar to SAHA, TST showed IC$_{50}$ values at nanomolar range and a selective index of at least 20 in different types of mammalian cells after 48 h of treatment. Cytotoxicity analysis after 120 h and using higher concentrations of SAHA and TST also showed that effective concentrations against parasite are innocuous to host cells, as the CC$_{50}$ obtained for SAHA [6,5 μM] and TST [29,9 μM] are 97 and 57 times higher than the IC$_{50}$ obtained for *T. gondii* (Supplementary data 3). SI obtained for SAHA [30] and TST [39] are higher than that reported for pyrimethamine against several cell lines, which varied from 5 to 17 (Adeyemi et al., 2020; Hopper et al., 2019; Spalenka et al., 2018). Further, the activity of SAHA and TST against *T. gondii* also showed IC$_{50}$ at the same range of pyrimethamine alone [0.12 μM] or when combined with sulfadiazine [0.067 μM] (Dubar et al., 2011; Martins-Duarte, 2006). A previous study with another selective inhibitor for HDAC6 in mammals, *N-hydroxy-4-[2-(3-methoxyphenyl) acetamido]benzamid*, also showed activity against the RH strain at a nanomolar range of concentration [IC$_{50}$ 0,35 μM and SI of 300 for the RH strain] (Loeuillet et al., 2018), indicating that selective compounds for HDAC6 in mammals are active against *T. gondii*. This is very interesting as *T. gondii* does not have any homologues for HDAC6, which suggests TST may inhibit another TgHDAC or might even have off target activity. Treatment with SAHA and TST drastically reduced *T. gondii* proliferation, even when drugs were removed from the medium. However, the presence of small

plaques containing parasites indicates residual parasite resistance to treatment. Both drugs also showed reasonable activity against the bradyzoite form of the EGS strain, but further studies will be necessary to verify if TST and SAHA are able to control the encystment of parasites and understand the effect on cell division and capacity to keep cyst viability. Our results support that known inhibitors of HDAC and its derivatives are interesting as drug leads for the designing of selective compounds against *T. gondii*. Although SAHA showed a selective effect against *T. gondii* this drug was developed against human HDAC and we cannot exclude potential toxicities. Future studies using recombinant proteins would give us the real idea of compound specificity for TgHDACs compared to human HDAC. Histones H3 and H4 in *T. gondii* are highly conserved through eukaryotic evolution and their acetylation upstream of constitutively expressed housekeeping genes was observed in both tachyzoites and bradyzoites (Nardelli et al., 2013; Saksouk et al., 2005). Analysis of H4 and H3 acetylation with SAHA and TST showed that both compounds act in H3 and H4 modification. Treatment with 1 μM TST increased the acetylation levels of H4 (Fig. 2G). Differently, decrease in H3 acetylation levels was pronounced after treatment with 1 μM TST (Fig. 3G). These effects in *T. gondii* nucleus might be associated to the degeneration of parasites seen by morphological analysis. Previous work by Bougdour et al. (2009) showed treatment of *T. gondii* with the HDAC3-specific inhibitor FR235222 also increased H4 acetylation (Bougdour et al., 2009). Interestingly, H3 modifications were also shown to be involved in stage-specific gene expression. TgHDAC3 is exclusively localized in the parasite nucleus and is recruited upstream of the bradyzoite-specific genes in tachyzoites (Saksouk et al., 2005; Nardelli et al., 2013). On the other hand, the HAT enzyme TgGCN5A, which exclusively acetylates histone H3 lysine 18 (Sullivan and Smith, 2000),
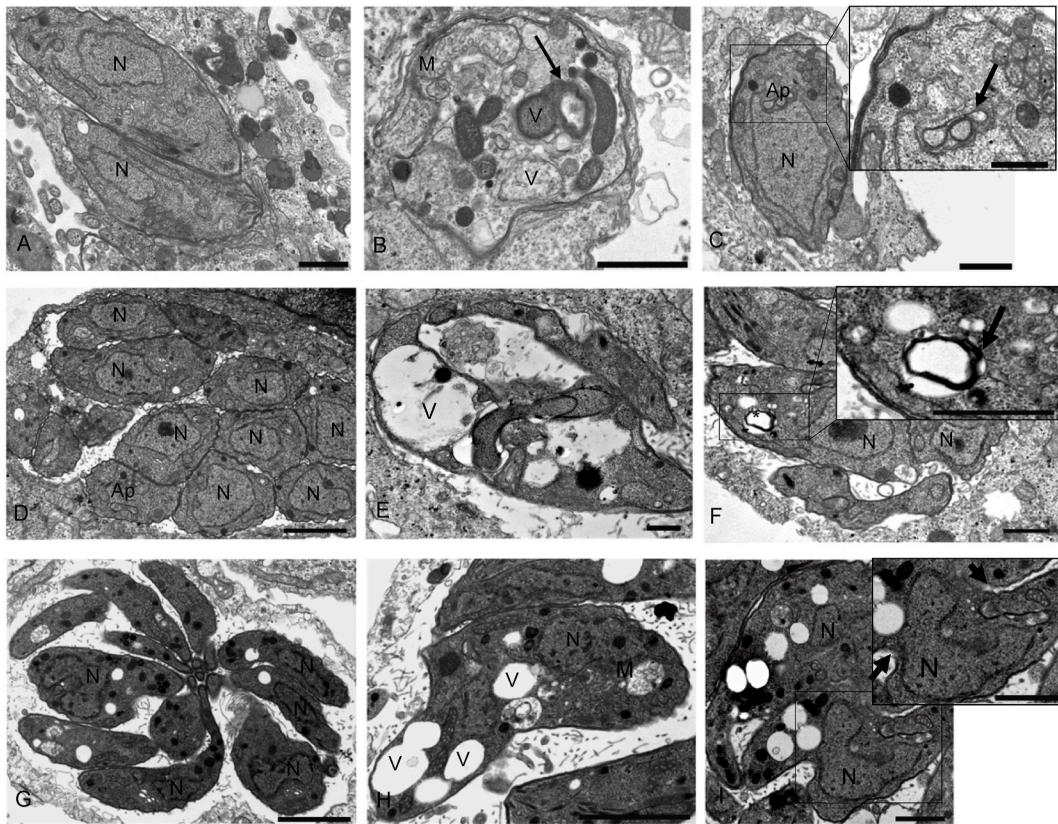
Fig. 8. Transmission electron microscopy of parasites treated with 3 μM TST or 0.2 μM SAHA for 12, 24 and 48 h. A, D and G Control parasites with typical ultrastructure after 12, 24 and 48 h. B–C Treatment with both compounds led to damages in the endodyogeny process and formation of large parasites. B, E and H TST-treated parasites presented mitochondria with disrupted crista and vacuolization of the cytoplasm. C After SAHA treatment, tachyzoites presented apicoplast with unusual morphology, apparent fragmentation (inset) and myelin-like structures in F (inset). I SAHA led to impaired new parasite individualization and consequently, the formation of a mass of parasites connected by the inner membrane complex (arrow inset). Nucleus **(N)**, Mitochondria **(M)**, Apicoplast **(Ap)**, Vacuole **(V)** Parasitophorous Vacuole **(PV)**. Scale bars: A, B, C, F and I = 1 μm; D = 2 μm; E = 0.5 μm; G, H = 2 μm. C, F and I insets = 1 μm.

acts at tachyzoite-specific promoters (Saksouk et al., 2005; Nardelli et al., 2013). Indeed, HAT TgGCN5B acetylates histone H3 lysine 9, 14, and 18 (Bhatti et al., 2006). TgHDAC3 and TgGCN5 cooperate in activating or repressing stage-specific genes (Saksouk et al., 2005; Vanagas et al., 2012). Thus, our data support TST and SAHA as targeting TgHDAC action either directly or indirectly, however off target activity cannot be excluded.

Interestingly, the treatment of *T. gondii* tachyzoites with SAHA affected correct apicoplast division and positioning during the process of the formation of new daughter cells. This phenomenon was observed frequently, and irregular organelle fragments could be observed in the several assays performed with ACP-YFP mutant parasites (Figs. 5 and 6). The apicoplast is a plastid-like organelle and contains a residual genome of 35 Kb; the presence of a prokaryote HU-like histone was already characterized in the apicoplast of *T. gondii* and *Plasmodium* (Ram et al., 2008; Reiff et al., 2012). In recent work, 400 acetylation sites were described in 274 proteins on *T. gondii* acetylome, with distinct cell distribution (Jeffers and Sullivan, 2012). Several proteins identified in *T. gondii* acetylome are apicoplast residents, among these: PDHE2 (dihydrolipoamide acetyltransferases of the pyruvate complex); TCP-1/Cpn60; acetyl-CoA carboxylase; 3-hydroxyalkyl-ACP dehydrogenase; and chaperones p23 (Jeffers and Sullivan, 2012), which are associated with type II fatty acid (FASII) biosynthesis, heme synthesis, and isoprenoid biosynthesis (Jelenska et al., 2002; Mazumdar et al., 2006). It is possible that enzymes inhibited by TST and SAHA may be involved in the PTM of the apicoplast proteins, however, the role of acetylation for the activity of the apicoplast proteins is not yet known. We cannot exclude that off-target effects were responsible for the

alterations in the apicoplast, as defects in parasite cell cycle could lead to apicoplast mislocalization.

On the other hand, TST, but not SAHA, affected *T. gondii* mitochondrial potential either directly or indirectly. *T. gondii* acetylome analysis also showed several mitochondrial proteins are acetylation-regulated sites, which might explain the remarkable decrease in mitochondrial membrane potential after treatment with TST. Jeffers and Sullivan showed that the porin voltage-dependent anion channel 1 (VDAC1) was one of the most-acetylated proteins in *T. gondi* (Jeffers and Sullivan, 2012). It is well known that one of the major and most abundant proteins in the mitochondrial outer membrane is voltage-dependent anion channel 1 (VDAC1), responsible for the passage of metabolites, nucleotides, and ions. VDAC1 is involved in the regulation of apoptosis, and its regulation is crucial not only for metabolic functions but for cell survival (Camara et al., 2017).

Alterations in cytoskeleton proteins possibly led to the formation of masses of damaged parasites and to the mislocalization of centrosomes of the mitotic spindle (Fig. 6). Furthermore, the correct assembling and extension of the inner membrane complex were also compromised (Fig. 7). Cytoskeleton proteins and intracellular vesicle transport proteins such as actin, actin depolymerization factor, α-tubulin, centrin, dynein, myosin A, profilin, and IMC-1 are also regulated by acetylation/ deacetylation (Jeffers and Sullivan, 2012), in the case of tubulin the enzyme HDAC6 in humans is known for its acetylation. However instead of an increase in the tubulin acetylation status, TST and SAHA treatment led to a decrease in the α-tubulin amount, which possibly affected microtubules in general and consequently cell division, thus we cannot exclude that the effects seen in cytoskeleton and *T. gondii* division were

due to a non-specific result caused by cell death. Differently in *P. falciparum*, SAHA increased α-tubulin transcription, affecting the cytoskeleton (Andrews et al., 2012).

Altogether, our results show that SAHA and TST in *T. gondii* possibly inhibit not just nuclear, but also other cytoplasmic HDACs, which are involved in the modification of proteins other than histones. Transcriptomic, proteomic and metabolomic studies must be done in treated parasites to indicate the future steps to be taken to achieve a better understanding of the interference of these inhibitors in the metabolism and cell cycle of this parasite. The effects of these inhibitors and the post-translational changes that they cause must be better explored in order to elect new pharmacological targets for the treatment of parasitic diseases with small host damage.

Declaration of competing interest

The authors declare that they have no known competing financial interests or personal relationships that could have appeared to influence the work reported in this paper.

Acknowledgements

Appendix A. Supplementary data

Supplementary data related to this article can be found at https://doi.org/10.1016/j.ijpddr.2020.12.003.

References

Adeyemi, O.S., Eseola, A.O., Plass, W., Atolani, O., Sugi, T., Han, Y., Batiha, G.E., Kato, K., Awakan, O.J., Olaolu, T.D., Nwonuma, C.O., Alejolowo, O., Owolabi, A., Rotimi, D., Kayode, O.T., 2020. Imidazole derivatives as antiparasitic agents and use of molecular modeling to investigate the structure–activity relationship. Parasitol. Res. 119, 1925–1941. https://doi.org/10.1007/s00436-020-06668-6.

Andrews, K., Haque, A., Jones, M.K., 2012. HDAC inhibitors in parasitic diseases. Immunol. Cell Biol. 90, 66–77. https://doi.org/10.1038/icb.2011.97.

Bhatti, M.M., Livingston, M., Mullapudi, N., Sullivan, W.J., 2006. Pair of unusual GCN5 histone acetyltransferases and ADA2 homologues in the Protozoan parasite toxoplasma gondii. Eukaryot. Cell 5, 62–76. https://doi.org/10.1128/EC.5.1.62-76.2006.

Bougdour, A., Maubon, D., Baldacci, P., Ortet, P., Bastien, O., Bouillon, A., Barale, J., Pelloux, H., Ménard, R., Hakimi, M., 2009. Drug inhibition of HDAC3 and epigenetic control of differentiation in Apicomplexa parasites. J. Exp. Med. 206, 953–966. https://doi.org/10.1084/jem.20082826.

Butler, K.V., Kalin, J., Brochier, C., Vistoli, G., Langley, B., Kozikowski, A.P., 2010. Rational design and simple chemistry yield a superior, neuroprotective HDAC6 inhibitor. Tubastatin A. J. Am. Chem. Soc. 132, 10842–10846. https://doi.org/10.1021/ja102758v.

Camara, A.K.S., Zhou, Y., Wen, P.-C., Tajkhorshid, E., Kwok, W.-M., 2017. Mitochondrial VDAC1: a key gatekeeper as potential therapeutic target. Front. Physiol. 8, 1–18. https://doi.org/10.3389/fphys.2017.00460.

Chua, M.J., Arnold, M.S.J., Xu, W., Lancelot, J., Lamotte, S., Späth, G.F., Prina, E., Pierce, R.J., Fairlie, D.P., Skinner-Adams, T.S., Andrews, K.T., 2017. Effect of clinically approved HDAC inhibitors on Plasmodium , Leishmania and Schistosoma parasite growth. Int. J. Parasitol. Drugs Drug Resist. 7, 42–50. https://doi.org/10.1016/j.ijpddr.2016.12.005.

Dai, Y., Faller, D.V., 2008. Transcription regulation by class III histone deacetylases (HDACs)-Sirtuins. Transl. Oncogenomics 3, 53–65. https://doi.org/10.4137/tog.s483.

Darkin-Rattray, S.J., Gurnett, A.M., Myers, R.W., Dulski, P.M., Crumley, T.M., Allocco, J. J., Cannova, C., Meinke, P.T., Colletti, S.L., Bednarek, M.A., Singh, S.B., Goetz, M.A.,

Dombrowski, A.W., Polishook, J.D., Schmatz, D.M., 1996. Apicidin: a novel antiprotozoal agent that inhibits parasite histone deacetylase. Proc. Natl. Acad. Sci. U.S.A. 93, 13143–13147. https://doi.org/10.1073/pnas.93.23.13143.

Dubar, F., Wintjens, R., Martins-Duarte, É.S., Vommaro, R.C., de Souza, W., Dive, D., Pierrot, C., Pradines, B., Wohlkonig, A., Khalife, J., Biot, C., 2011. Esterprodrugs of ciprofloxacin as DNA-gyrase inhibitors: synthesis, antiparasitic evaluation and docking studies. Medchemcomm 2, 430–435. https://doi.org/10.1039/C1MD00022E.

Dubey, J.P., Lago, E.G., Gennari, S.M., Su, C., Jones, J.L., 2012. Toxoplasmosis in humans and animals in Brazil: high prevalence, high burden of disease, and epidemiology. Parasitology 139, 1375–1424. https://doi.org/10.1017/S0031182012000765.

Engel, J.A., Jones, A.J., Avery, V.M., Sumanadasa, S.D.M., Ng, S.S., Fairlie, D.P., Adams, T.S., Andrews, K.T., 2015. Profiling the anti-protozoal activity of anti-cancer HDAC inhibitors against Plasmodium and Trypanosoma parasites. Int. J. Parasitol. Drugs Drug Resist. 5, 117–126. https://doi.org/10.1016/j.ijpddr.2015.05.004.

Fioravanti, R., Mautone, N., Rovere, A., Rotili, D., Mai, A., 2020. Targeting histone acetylation/deacetylation in parasites: an update (2017–2020). Curr. Opin. Chem. Biol. 57, 65–74. https://doi.org/10.1016/j.cbpa.2020.05.008.

Gelb, M.H., Van Voorhis, W.C., Buckner, F.S., Yokoyama, K., Eastman, R., Carpenter, E. P., Panethymitaki, C., Brown, K.A., Smith, D.F., 2003. Protein farnesyl and N-myristoyl transferases: piggy-back medicinal chemistry targets for the development of antitrypanosomatid and antimalarial therapeutics. Mol. Biochem. Parasitol. 126, 155–163. https://doi.org/10.1016/S0166-6851(02)00282-7.

Grant, S., Easley, C., Kirkpatrick, P., 2007. Vorinostat. Nat. Rev. Drug Discov. 6, 21–22. https://doi.org/10.1038/nrd2227.

Halonen, S.K., Weiss, L.M., 2013. Toxoplasmosis, pp. 125–145. https://doi.org/10.1016/B978-0-444-53490-3.00008-X.

Heimburg, T., Chakrabarti, A., Lancelot, J., Marek, M., Melesina, J., Hauser, A.-T., Shaik, T.B., Duclaud, S., Robaa, D., Erdmann, F., Schmidt, M., Romier, C., Pierce, R. J., Jung, M., Sippl, W., 2016. Structure-based design and synthesis of novel inhibitors targeting HDAC8 from schistosoma mansoni for the treatment of schistosomiasis. J. Med. Chem. 59, 2423–2435. https://doi.org/10.1021/acs.jmedchem.5b01478.

Hopper, A.T., Brockman, A., Wise, A., Gould, J., Barks, J., Radke, J.B., Sibley, L.D., Zou, Y., Thomas, S., 2019. Discovery of selective toxoplasma gondii dihydrofolate reductase inhibitors for the treatment of toxoplasmosis. J. Med. Chem. 62, 1562–1576. https://doi.org/10.1021/acs.jmedchem.8b01754.

Hubbert, C., Guardiola, A., Shao, R., Kawaguchi, Y., Ito, A., Nixon, A., Yoshida, M., Wang, X.-F., Yao, T.-P., 2002. HDAC6 is a microtubule-associated deacetylase. Nature 417, 455–458. https://doi.org/10.1038/417455a.

Jeffers, V., Sullivan, W.J., 2012. Lysine acetylation is widespread on proteins of diverse function and localization in the Protozoan parasite toxoplasma gondii. Eukaryot. Cell 11, 735–742. https://doi.org/10.1128/EC.00088-12.

Jelenska, J., Sirikhachornkit, A., Haselkorn, R., Gornicki, P., 2002. The carboxyltransferase activity of the apicoplast acetyl-CoA carboxylase of toxoplasma gondii is the target of aryloxyphenoxypropionate inhibitors. J. Biol. Chem. 277, 23208–23215. https://doi.org/10.1074/jbc.M200455200.

Jones-Brando, L., Torrey, E.F., Yolken, R., 2003. Drugs used in the treatment of schizophrenia and bipolar disorder inhibit the replication of Toxoplasma gondii. Schizophr. Res. 62, 237–244. https://doi.org/10.1016/s0920-9964(02)00357-2.

Lian, H., Roy, E., Zheng, H., 2016. Protocol for primary microglial culture preparation. Bio-Protoc 6, 1–10. https://doi.org/10.21769/bioprotoc.1989.

Loeuillet, C., Touquet, B., Oury, B., Eddaikra, N., Pons, J.L., Guichou, J.F., Labesse, G., Sereno, D., 2018. Synthesis of aminophenylhydroxamate and aminobenzylhydroxamate derivatives and in vitro screening for antiparasitic and histone deacetylase inhibitory activity. Int. J. Parasitol. Drugs Drug Resist. 8, 59–66. https://doi.org/10.1016/j.ijpddr.2018.01.002.

Martins-Duarte, É.D.S., De Souza, W., Vommaro, R.C., 2008. Itraconazole affects Toxoplasma gondii endodyogeny. FEMS Microbiol. Lett. 282, 290–298. https://doi.org/10.1111/j.1574-6968.2008.01130.x.

Martins-Duarte, E.S., 2006. Antiproliferative activities of two novel quinuclidine inhibitors against Toxoplasma gondii tachyzoites in vitro. J. Antimicrob. Chemother. 58, 59–65. https://doi.org/10.1093/jac/dkl180.

Mazumdar, J., Wilson, E.H., Masek, K., Hunter, C.A., Striepen, B., 2006. Apicoplast fatty acid synthesis is essential for organelle biogenesis and parasite survival in Toxoplasma gondii. Proc. Natl. Acad. Sci. Unit. States Am. 103, 13192–13197. https://doi.org/10.1073/pnas.0603391103.

Michan, S., Sinclair, D., 2007. Sirtuins in mammals: insights into their biological function. Biochem. J. 404, 1–13. https://doi.org/10.1042/BJ20070140.

Montoya, J., Liesenfeld, O., 2004. Toxoplasmosis. Lancet 363, 1965–1976. https://doi.org/10.1016/S0140-6736(04)16412-X.

Nardelli, S.C., Che, F.Y., Silmon de Monerri, N.C., Xiao, H., Nieves, E., Madrid-Aliste, C., Angel, S.O., Sullivan, W.J., Angeletti, R.H., Kim, K., Weiss, L.M., 2013. The histone code of Toxoplasma gondii comprises conserved and unique posttranslational modifications. mBio 4. https://doi.org/10.1128/mBio.00922-13.

North, B.J., Verdin, E., 2004. Sirtuins: Sir2-related NAD-dependent protein deacetylases. Genome Biol. 5, 224. https://doi.org/10.1186/gb-2004-5-5-224.

Nwaka, S., Hudson, A., 2006. Innovative lead discovery strategies for tropical diseases. Nat. Rev. Drug Discov. 5, 941–955. https://doi.org/10.1038/nrd2144.

Oliveira Santos, J., Zuma, A.A., de Luna Vitorino, F.N., da Cunha, J.P.C., de Souza, W., Motta, M.C.M., 2019. Trichostatin A induces Trypanosoma cruzi histone and tubulin acetylation: effects on cell division and microtubule cytoskeleton remodelling. Parasitology 146, 543–552. https://doi.org/10.1017/S0031182018001828.

Paredes-Santos, T.C., Martins-Duarte, E.S., Vitor, R.W.A., de Souza, W., Attias, M., Vommaro, R.C., 2013. Spontaneous cystogenesis in vitro of a Brazilian strain of

Toxoplasma gondii. Parasitol. Int. 62, 181–188. https://doi.org/10.1016/j.parint.2012.12.003.

Ram, E.V.S.R., Naik, R., Ganguli, M., Habib, S., 2008. DNA organization by the apicoplast-targeted bacterial histone-like protein of Plasmodium falciparum. Nucleic Acids Res. 36, 5061–5073. https://doi.org/10.1093/nar/gkn483.

Reiff, S.B., Vaishnava, S., Striepen, B., 2012. The HU protein is important for apicoplast genome maintenance and inheritance in toxoplasma gondii. Eukaryot. Cell 11, 905–915. https://doi.org/10.1128/EC.00029-12.

Roberts, F., McLeod, R., 1999. Pathogenesis of toxoplasmic retinochoroiditis. Parasitol. Today 15, 51–57. https://doi.org/10.1016/S0169-4758(98)01377-5.

Ruefli, A.A., Ausserlechner, M.J., Bernhard, D., Sutton, V.R., Tainton, K.M., Kofler, R., Smyth, M.J., Johnstone, R.W., 2001. The histone deacetylase inhibitor and chemotherapeutic agent suberoylanilide hydroxamic acid (SAHA) induces a cell-death pathway characterized by cleavage of Bid and production of reactive oxygen species. Proc. Natl. Acad. Sci. Unit. States Am. 98, 10833–10838. https://doi.org/10.1073/pnas.191208598.

Ruijter, A.J.M. de, van Gennip, A.H., Caron, H.N., Kemp, S., van Kuilenburg, A.B.P., 2003. Histone deacetylases (HDACs): characterization of the classical HDAC family. Biochem. J. 370, 737–749. https://doi.org/10.1042/bj20021321.

Saksouk, N., Bhatti, M.M., Kieffer, S., Smith, A.T., Musset, K., Garin, J., Sullivan, W.J., Cesbron-Delauw, M.-F., Hakimi, M.-A., 2005. Histone-modifying complexes regulate gene expression pertinent to the differentiation of the Protozoan parasite toxoplasma gondii. Mol. Cell Biol. 25, 10301–10314. https://doi.org/10.1128/MCB.25.23.10301-10314.2005.

Sodji, Q., Patil, V., Jain, S., Kornacki, J.R., Mrksich, M., Tekwani, B.L., Oyelere, A.K., 2014. The antileishmanial activity of isoforms 6- and 8-selective histone deacetylase inhibitors. Bioorg. Med. Chem. Lett 24, 4826–4830. https://doi.org/10.1016/j.bmcl.2014.08.060.

Spalenka, J., Escotte-Binet, S., Bakiri, A., Hubert, J., Renault, J.H., Velard, F., Duchateau, S., Aubert, D., Huguenin, A., Villena, I., 2018. Discovery of new

inhibitors of toxoplasma gondii via the pathogen box. Antimicrob. Agents Chemother. 62 https://doi.org/10.1128/AAC.01640-17.

Stenzel, K., Chakrabarti, A., Melesina, J., Hansen, F.K., Lancelot, J., Herkenhöhner, S., Lungerich, B., Marek, M., Romier, C., Pierce, R.J., Sippl, W., Jung, M., Kurz, T., 2017. Isophthalic acid-based HDAC inhibitors as potent inhibitors of HDAC8 from schistosoma mansoni. Arch. Pharm. (Weinheim) 350. https://doi.org/10.1002/ardp.201700096, 1700096.

Striepen, B., Crawford, M.J., Shaw, M.K., Tilney, L.G., Seeber, F., Roos, D.S., 2000. The plastid of toxoplasma gondii is divided by association with the centrosomes. J. Cell Biol. 151, 1423–1434. https://doi.org/10.1083/jcb.151.7.1423.

Strobl, J.S., Cassell, M., Mitchell, S.M., Reilly, C.M., Lindsay, D.S., 2007. SCRIPTAID and suberoylanilide hydroxamic acid are histone deacetylase inhibitors with potent anti–toxoplasma gondii activity IN vitro. J. Parasitol. 93, 694–700. https://doi.org/10.1645/GE-1043R.1.

Sullivan, W.J., Smith, C.K., 2000. Cloning and characterization of a novel histone acetyltransferase homologue from the protozoan parasite Toxoplasma gondii reveals a distinct GCN5 family member. Gene 242, 193–200. https://doi.org/10.1016/S0378-1119(99)00526-0.

Suraweera, A., O'Byrne, K.J., Richard, D.J., 2018. Combination therapy with histone deacetylase inhibitors (HDACi) for the treatment of cancer: achieving the full therapeutic potential of HDACi. Front. Oncol. 8, 1–15. https://doi.org/10.3389/fonc.2018.00092.

Vanagas, L., Jeffers, V., Bogado, S.S., Dalmasso, M.C., Sullivan, W.J., Angel, S.O., 2012. Toxoplasma histone acetylation remodelers as novel drug targets. Expert Rev. Anti Infect. Ther. 10, 1189–1201. https://doi.org/10.1586/eri.12.100.

Zhang, Y., Au, Q., Zhang, M., Barber, J.R., Ng, S.C., Zhang, B., 2009. Identification of a small molecule SIRT2 inhibitor with selective tumor cytotoxicity. Biochem. Biophys. Res. Commun. 386, 729–733. https://doi.org/10.1016/j.bbrc.2009.06.113.

Zuma, A.A., De Souza, W., Souza, W. de, 2018. Histone deacetylases as targets for antitrypanosomal drugs. Futur. Sci. OA 4, FSO325. https://doi.org/10.4155/fsoa-2018-0037.